SLAC – PUB – 4150
December 1986
(M)

SLAC-PUB--4150

DE87 010320

HADRON CASCADES PRODUCED BY ELECTROMAGNETIC CASCADES*

W. R. NELSON and T. M. JENKINS

Stanford Linear Accelerator Center
Stanford University, Stanford, California 94305

J. RANFT

Sektion Physik, Karl-Marx-Universität
Leipzig, German Democratic Republic

ABSTRACT

A method for calculating high energy hadron cascades induced by multi-GeV electron and photon beams is described. Using the EGS4 computer program, high energy photons in the EM shower are allowed to interact hadronically according to the vector meson dominance (VMD) model, facilitated by a Monte Carlo version of the dual multistring fragmentation model which is used in the hadron cascade code FLUKA. The results of this calculation compare very favorably with experimental data on hadron production in photon-proton collisions and on the hadron production by electron beams on targets (i.e., yields in secondary particle beam lines). Electron beam induced hadron star density contours are also presented and are compared with those produced by proton beams. This FLUKA-EGS4 coupling technique could find use in the design of secondary beams, in the determination high energy hadron source terms for shielding purposes, and in the estimation of induced radioactivity in targets, collimators and beam dumps.

INTRODUCTION

In a hadron cascade, a substantial fraction of the energy is deposited in the medium by electromagnetic showers, induced primarily by decaying π^0 mesons. Consequently, hadron cascade calculations generally account for the EM cascade in some manner, although the inverse is not necessarily true—*i.e.*, the dominant features of EM showers induced by electron or photon beams can be understood from pure electron-photon cascade calculations without coupling to hadron cascade calculations, or even including hadron production as a loss mechanism.

Hadron cascade calculations have been performed mainly to show radiation effects around high energy accelerators (1) and, in recent years, to study the performance of hadron calorimeters. On the other hand, electromagnetic cascade calculations (2) have proved to be tremendously useful in the design of electron accelerators and storage rings, and even essential for the proper design of electron-photon calorimeters. They have been used to a much lesser extent in the estimation of radiation effects around high energy accelerators.

* Work supported by the Department of Energy, contract DE – AC03 – 76SF00515.

Invited talk presented at the Midyear Symposium of the
Health Physics Society, Reno, Nevada, February 8–12, 1987

CONF-870219--11

With the construction of electron accelerators of higher and higher energies, such as the LEP machine at CERN and the SLC at the Stanford Linear Accelerator Center, there is increasing interest in being able to perform coupled EM-hadronic cascade calculations for a number of reasons, including the study of radiation effects around these machines. One of the first studies involving photohadron production was done by DeStaebler (3) in the early 1960s, which covered the energy range from tens of GeV down to the giant resonance region. This work has found extensive use in shielding both the Stanford two-mile electron linac and the various experiments at that facility (4).

As will be demonstrated in this paper, we are now better equipped with sophisticated Monte Carlo codes and with a more complete understanding of the physics that occurs at energies above 1 GeV. The purpose of the present work, therefore, is to study the high energy hadron component induced by photons in the GeV energy region. There is a second, less abundant, hadron component induced by deep inelastic electron-hadron interactions which is not, however, included in this study.

We first describe the vector meson dominance (VMD) model that we use for the hadronic interactions of high energy photons with nuclei. This is followed by a brief discussion of the dual multistring fragmentation model that is used in the FLUKA (5,6) hadron cascade code in order to generate photon-hadron and photon-nucleus events in the Monte Carlo calculation of the hadron cascade. The EM shower produced by electron or photon beams is treated by means of the EGS4 code (2) and the implementation of the hadronic interactions of photons in the coupled hadron-electromagnetic cascade code (FLUKA-EGS) is described. Finally, we give results of hadron cascade calculations with incident electron beams and compare the hadron yields to experimental data.

HADRONIC INTERACTIONS OF PHOTONS AND THE VMD MODEL

In order to include the hadronic interaction of photons into hadron-electromagnetic cascade calculations, we need

(*i*) the total hadronic cross sections of photons in order to determine the hadronic interaction probabilities of the photons, and

(*ii*) a model to simulate inelastic photon-nucleus events.

The hadronic cross sections of photons are well described in the framework of the VMD model as described, for instance, in the review papers of Bauer, Spital, Yennie and Pipkin (7) and Schildknecht (8). Above 2 GeV we describe the total inelastic photon nucleon cross sections by the simple parametrization (7)

$$\begin{aligned} \sigma_{\gamma p} &= 99.8 + 57.0/\sqrt{E_\gamma}\ [\mu b] \\ \sigma_{\gamma n} &= 98.5 + 45.2/\sqrt{E_\gamma}\ [\mu b] \end{aligned} \qquad (1)$$

where E_γ is the photon energy in GeV. Below 2 GeV the photon-nucleon cross sections show a considerable resonance structure for which, in the present study, we use the experimental data as collected, for instance, by the Particle Data Group (9) or by Bauer et al (7).

The interaction of photons on nuclear targets can be described by using an effective nuclear mass number A_{eff}

$$\frac{A_{eff}}{A} = \frac{\sigma_{\gamma A}}{Z\sigma_{\gamma p} + (A - Z)\sigma_{\gamma n}} \tag{2}$$

The ratio A_{eff}/A has been determined experimentally. Above 2 GeV the data are well described by a constant ratio $A_{eff}/A \approx 0.7$ - 0.8. At lower energies the ratio rises to $A_{eff}/A \rightarrow 1$ (7).

According to the VMD model, the photon interacts hadronically as a vector meson ρ, ω or ϕ. While ρ and ω occur with equal probability, the ϕ vector-meson contributes only about 8% to the cross section. What we need is a model describing particle production for inelastic hadron-nucleon and hadron-nucleus collisions, where the projectile hadrons are vector mesons. This model will be discussed next.

DUAL MULTISTRING FRAGMENTATION MODEL AND FLUKA

The hadron cascade code FLUKA (5,6) uses a Monte Carlo version of the multistring fragmentation model due to Ranft and Ritter (10), which is based on the dual-topological-unitarization (DTU) scheme following earlier work of Capella et al (11). Suffice it to say that in this model, which is described in more detail elsewhere (12), only the quark composition of the participating hadrons has to be known; therefore, we can calculate inelastic events even in ρ^0-nucleus, ω-nucleus and ϕ-nucleus collisions. In addition to this dominant nondiffractive component of particle production, we include the single diffractive component of hadron-hadron scattering for both target and projectile fragmentation, which can also be described by the Monte Carlo chain decay model (13).

For the fragmentation of the quark-antiquark and quark-diquark chains, which occur in these models, we use a Monte Carlo chain decay model (14), which was originally tested against data from hadron production in e^+e^- collisions (15).

COMPARISON OF PHOTON-HADRON PRODUCTION WITH EXPERIMENT

In Fig. 1 we compare the Feynman-x distribution, $F(x)$, of π^- mesons produced in photon-proton collisions with π^- production in $\pi^\pm$-proton collisions. Feynman-x is the fraction of the longitudinal momentum of the primary carried by the secondary (in the CM system). Feynman-x values range from -1 (secondary has momentum of target) to +1 (secondary has momentum of primary); particles at rest in the CM have Feynman-x=0. It is evident from the experimental data (16) plotted in Fig. 1a, as well as from our calculations plotted in Fig. 1b, that particle production in photon-hadron and pion-hadron collisions is very similar indeed.

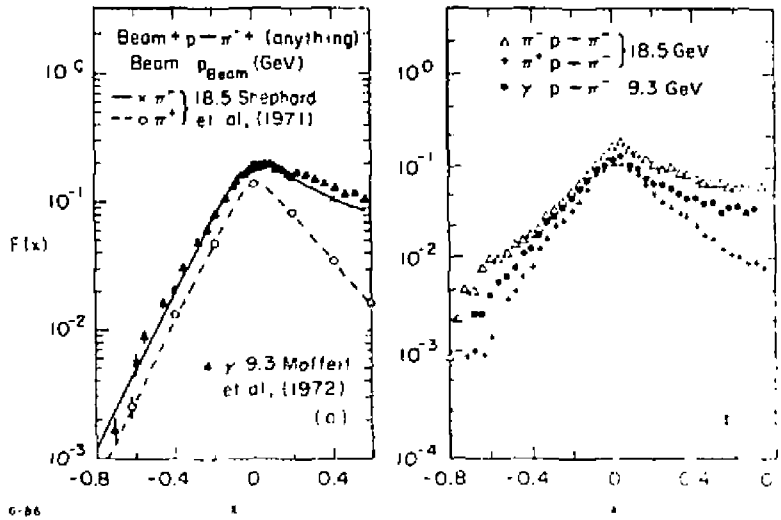

Fig. 1. Comparison of Feynman-x distributions of π^- mesons produced in $\pi^+ p$ and γp collisions: a) Experimental data (16). b) Calculations according to the dual multistring fragmentation model.

We next compare with more recent data (17) concerning the photoproduction of neutral strange hadrons in 20 GeV photon-proton collisions. In Table 1 we compare the total multiplicities of produced neutral strange hadrons and find very good agreement.

Table 1

Λ, $\bar{\Lambda}$ and K^0_s Production in 19.5 GeV γ-Proton Interactions.

Multiplicity	Experiment (17)	Model
n_Λ	0.054 ± 0.002	0.044 ± 0.004
$n_{\bar{\Lambda}}$	0.0037 ± 0.0003	0.0044 ± 0.001
$n_{K^0_s}$	0.093 ± 0.003	0.099 ± 0.004

In Fig. 2 we compare the Feynman-x distribution of produced Λ and $\bar{\Lambda}$ hyperons and K^0_s mesons. We find very good agreement in the photon fragmentation region but some differences concerning Λ hyperon production in the proton fragmentation region.

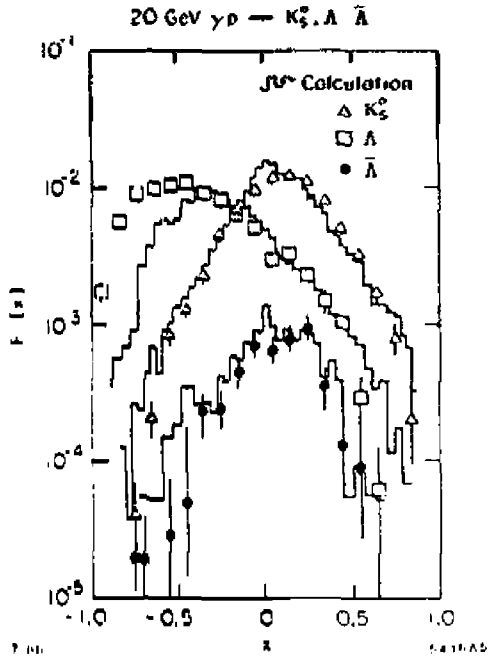

Fig. 2. Comparisons of Λ, $\bar{\Lambda}$ and K^0_S produced in 20 GeV γp collisions (17) with the predictions of the dual multistring fragmentation model.

In a separate publication (12), we have also made comparisons with recent data (18) on particle production in diffractive photon-proton collisions in the photon fragmentation region. We conclude that the model also describes the diffractive component of particle production in photon-hadron collisions quite well. We conclude from all these comparisons that the model describes the data on hadron production in the photon fragmentation region well enough to be safely applied in hadron-electromagnetic cascade calculations.

COUPLING FLUKA AND EGS4 USING THE VMD MODEL

The hadronic interaction cross sections of photons are typically a factor 100 or more smaller than the pair production and Compton scattering cross sections. Therefore, a straight forward analog Monte Carlo simulation of the hadronic interactions of photons occurring in the electromagnetic cascade would lead to very small hadron fluences. As a result, we have elected to apply biasing and weighting techniques as follows.

We consider each photon with sufficient energy for an inelastic hadronic interaction (*i.e.*, $E_\gamma \gtrsim 200$ MeV). From the simulation in EGS, we know the place where the photon was produced (or entered the material from outside), its direction, and its distance before

interacting (or leaving the material). Along this distance, D_γ, we calculate the hadronic interaction probability of the photon

$$\omega_\gamma = 1 - \exp(-D_\gamma/\lambda_{\gamma h}) \ , \qquad (3)$$

where $\lambda_{\gamma h}$ is the hadronic interaction length of the photon in the material. We proceed by appropriately decreasing the weight of the photon in EGS and add to the stack of hadrons in FLUKA a hadron with the proper quark-anti quark composition of a vector meson with the weight ω_γ. This hadron is furthermore required to interact along the distance D_γ.

In order to obtain good statistics for the hadron production in such calculations, it is advisable to set the energy thresholds (cutoffs) for photons and electrons as high as possible, and also to use the leading particle bias option of EGS. In this option, only one particle is retained at each vertex (i.e., the one with the higher energy), and a new weight is appropriately assigned (e.g., see Ref. (19)).

RESULTS OF THE CALCULATION AND COMPARISON WITH EXPERIMENT

The yields of secondary hadrons from 18 GeV electrons on a 0.3 radiation length beryllium target were measured 18 years ago at SLAC (20). In Figs. 3a and b, we compare (on an absolute basis) the π^+ yields at different momenta and production angles with the results of the coupled FLUKA-EGS calculation.

Although the calculated yields are slightly lower than the measured ones, our method essentially reproduces the measured data. Monte Carlo calculations of this type are difficult because of statistical limitations, particularly when they involve scoring in two-dimensions (e.g., momentum and angle). Hence, kaon and anti-nucleon results are not presented at this time.

Encouraged by this agreement, we calculate the hadron cascades initiated by electron beams in blocks of iron, aluminium and water. We present the results of the calculations in the form of hadron star densities (stars/cm^3), as well as the total number of hadron stars (per incident beam particle and per GeV beam incident energy). We compare these values in the case of iron with the results obtained for primary proton beams.

In Table 2, we present the total number of hadron stars produced in a large block of material, both per incident projectile (electron or proton) and per GeV of incident energy.

In the case of iron, a factor of 300 to 600 fewer stars are produced per electron than per proton. In lighter materials, where the radiation length becomes comparable to the hadronic collision length, the number of hadron stars generated per incident electron increases accordingly.

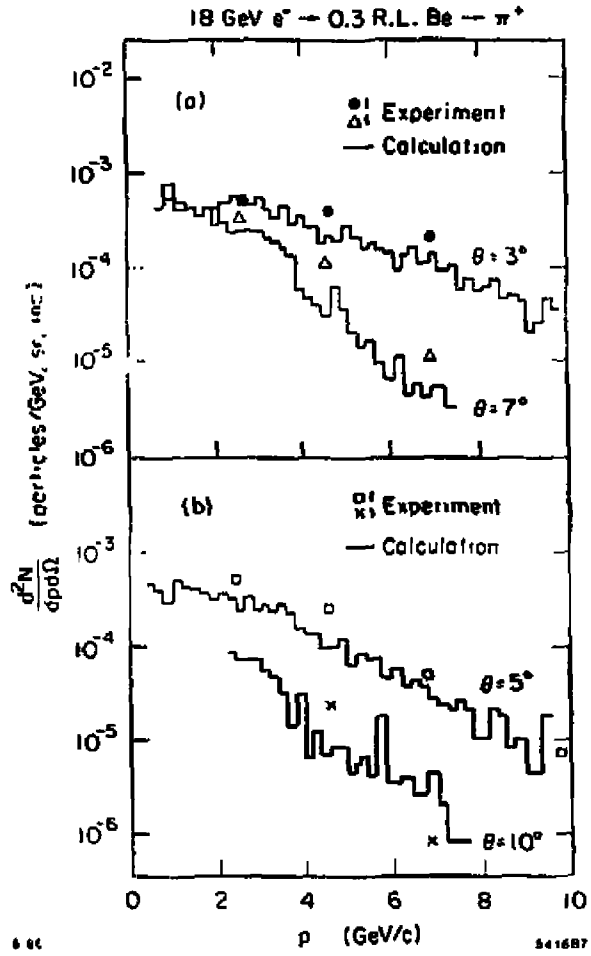

Fig. 3. Comparison of π^+ yields from a 0.3 radiation length Be target hit by an 18 GeV electron beam.

Table 2.

Total Number of Hadron Stars Produced in the Hadron Cascade.

Beam	Target	Beam Energy [GeV]	Stars/Projectile	Stars/GeV Inc. Energy
p	Fe	10	20	2.
		20	39.8	1.99
		50	81	1.65
		100	140	1.40
e	Fe	10	0.032	0.0032
		20	0.075	0.0038
		50	0.21	0.0042
		100	0.499	0.0050
e	Al	10	0.058	0.0058
		20	0.14	0.0070
		50	0.38	0.0076
		100	0.85	0.0085
e	H_2O	10	0.082	0.0082
		20	0.19	0.0085
		50	0.54	0.011
		100	1.2	0.012

The total number of hadron stars produced within an iron slab of thickness Δz = 1 cm is plotted in Fig. 4 as function of z for both incident electrons and protons. The longitudinal star density profile curves are seen to be different for the two incident projectile cases. For hadrons, the star density builds up slowly, reaching its maximum at a depth of several hadronic absorption lengths. For incident electrons, on the other hand, the buildup is more rapid and occurs at a depth of the order of a radiation length. The slope of the attenuation at large depths looks rather similar for hadron and electron projectiles. Also, the shape of the transverse attenuation of the hadron cascade seems to be the same in both cases.

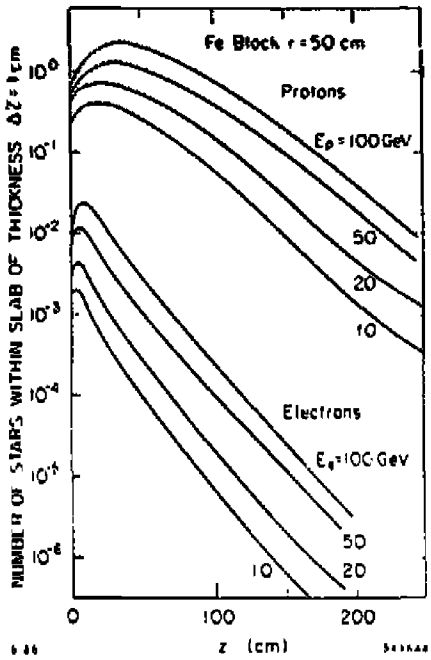

Fig. 4. Comparison of the hadron cascade inside a large (z = 250 cm, r = 50 cm) iron cylinder hit by proton and electron beams with energies between 10 and 100 GeV.

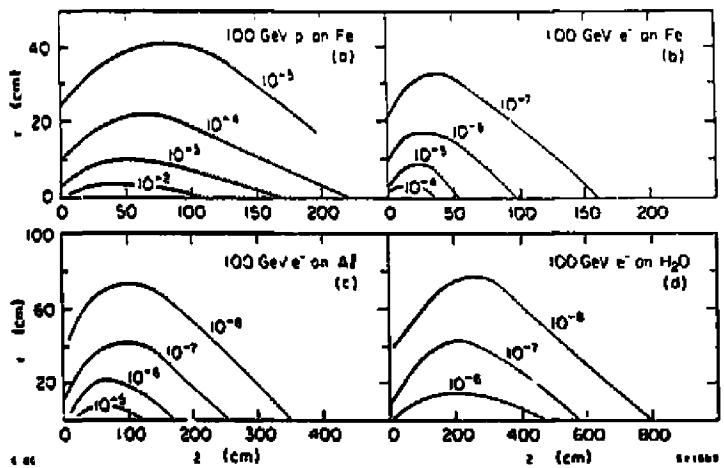

Fig. 5. Curves of constant hadron star density (stars/cm³/inc) for proton and electron beams striking Fe, Al, and water targets.

In Fig. 5a through d, we plot hadron star densities in cylindrical blocks of material in the form of contours of equal star densities. For comparison, we include the case of a proton beam hitting an iron block, where again the differences between the cascades induced by hadron and electron projectiles becomes apparent. Star density curves of this type have been shown to be useful in estimating the dose equivalent (rate) from residual radioactivity generated by the hadron cascade (21-23).

CONCLUDING REMARKS

A method for coupling electromagnetic and hadronic cascades using the EGS4 and FLUKA codes, respectively, has been presented. The photoproduction of hadrons by the bremsstrahlung photons in the EM cascade has been included by means of the vector meson dominance (VMD) model. This method of coupling is able to give essentially correct results for hadron stars and hadron fluences induced by electron or photon beams in blocks of material. As expected, the electron induced hadron cascades are suppressed by about a factor of 300 to 600 compared to those initiated by incident hadrons themselves. Also, the radial and longitudinal profiles (per beam energy) differ for the two particle types.

This FLUKA-EGS4 coupling technique could find use in the design of secondary beams, in the determination of high energy hadron source terms for shielding studies, as well as in the estimation of induced radioactivity in devices such as targets, collimators, and beam dumps. The induced activity, produced in this case by high energy interactions, can be added to that created by the more abundant giant resonance excitation.

Acknowledgement

One of the authors (J. R.) acknowledges the hospitality and support of both the Radiation Physics Group at SLAC and the Radiation Protection Group at CERN where much of this work was done.

References

1. J. Ranft, Particle Accelerators 3, p. 129 (1972).
2. W. R. Nelson, H. Hirayama and D. W. O. Rogers, "The EGS4 Code System", Stanford Linear Accelerator Center Report Number SLAC-265 (1985).
3. H. DeStaebler, Jr., "Transverse Radiation Shielding for the Stanford Two-Mile Accelerator", Stanford Linear Accelerator Center Report Number SLAC-9 (1962).
4. H. DeStaebler, T. M. Jenkins, and W. R. Nelson, "Shielding and Dosimetry", Chapter 26 in THE STANFORD TWO-MILE ACCELERATOR edited by R. B. Neal (W. A. Benjamin, Inc., New York, 1968).
5. P. A. Aarnio, J. Ranft and G. R. Stevenson, "A Long Writeup of the FLUKA82 Program", CERN Divisional Report Number TIS-RP/106 Rev (1984).
6. P. A. Aarnio, A. Fasso, H. J. Moehring, J. Ranft and G. R. Stevenson, "FLUKA86 Users Guide", CERN Divisional Report Number TIS-RP/168 (1986).

7. T. H. Bauer, R. D.Spital, D. R. Yennie and F. M. Pipkin, Rev. Mod. Phys. 50, p. 261 (1978).

8. D. Schildknecht, Springer Tracts in Modern Physics 63, p. 57 (1972).

9. M. Roos, F. C. Porter, M. Aguilar-Benitez, L. Montanet, Ch. Walck, R. L. Crawford, R. L. Kelly, A. Rittenberg, T. G. Trippe, C. G. Wohl, G. P. Yost, T. Shimada, M. J. Losty, G. P. Gopal, R. E. Hendrick, R. E. Shrock, R. Frosch, L. D. Roper and B. Armstrong, Phys. Lett. 111B, p. 1 (1982).

10. J. Ranft and S. Ritter, Z. Phys. C20, p. 347 (1983); Z. Phys. C27, p. 413 (1985); Z. Phys. C27, p. 569 (1985).

11. A. Capella, U. Sukhatme, C. I. Tan and J. Tran Thanh Van, Phys. Lett. 81B, 68 (1979); A. Capella and J. Tran Thanh Van, Phys. Lett. 93B, p. 146 (1980); Z. Phys. C10, p. 249 (1981).

12. J. Ranft and W. R. Nelson, "Hadron Cascades Induced by Electron and Photon Beams in the GeV Energy Range", Stanford Linear Accelerator Report Number SLAC-PUB-3959 (1986), submitted to Nucl. Instr. and Meth.

13. J. Ranft, to be published in Z. Phys.

14. S. Ritter, Comput. Phys. Commun. 31, p. 393 (1984).

15. S. Ritter and J. Ranft, Acta. Phys. Pol. B11, p. 259 (1980); S. Ritter, Z. Phys. C26, p. 27 (1982).

16. W. D. Shephard et al, Phys. Rev. Lett. 27, p. 1164 (1971); K. C. Moffeit et al, Phys. Rev. Lett. D5, p. 1603 (1972).

17. K. Abe et al, Phys. Rev. D32, p. 2869 (1985).

18. S. Bhadra et al, Colorado University Report Number COLO-HEP-104 (1985), submitted to Phys. Rev. Lett.

19. J. Ranft, H. J. Mochring, T. M. Jenkins, and W. R. Nelson, "The Hadron Cascade Code FLUKA82, Setup and Coupling With EGS4 at SLAC", Stanford Linear Accelerator Center Report Number SLAC-TN-86-3 (1986).

20. A. M. Boyarski, F. Bulos, W. Busra, R. Diebold, S. D. Ecklund, G. E. Fischer, J. R. Rees and B. Richter, "Yields of Secondary Particles from 18 GeV Electrons", in SLAC Users Handbook (1971); Phys. Rev. Lett. 18, p. 363 (1967).

21. G. R. Stevenson, "Dose Equivalent Per Star in Hadron Cascade Calculations", CERN Divisional Report Number TIS-RP/173 (1986);

22. A. Van Ginneken and M. Awschalom, HIGH ENERGY PARTICLE INTERACTIONS IN LARGE TARGETS; VOLUME 1. HADRONIC CASCADES, SHIELDING, ENERGY DEPOSITION (Fermi National Accelerator Laboratory, Batavia, Illinois, 1975).

23. J. Ranft, "The FLUKA and KASPRO Hadronic Cascade Codes", Chapter 22 in COMPUTER TECHNIQUES IN RADIATION TRANSPORT AND DOSIMETRY edited by W. R. Nelson and T. M. Jenkins (Plenum Press, New York, 1980).